Mechanisms of Ageing and Development 183 (2019) 111151

Contents lists available at ScienceDirect

Mechanisms of Ageing and Development

journal homepage: www.elsevier.com/locate/mechagedev

Glycoanalysis of the placental membrane glycoproteins throughout placental development

Dragana Robajac[a,*], Romana Masnikosa[a,1], Marek Nemčovič[b], Martina Križáková[b], Ľudmila Belická Kluková[b], Peter Baráth[b], Jaroslav Katrlík[b], Olgica Nedić[a]

[a] Institute for the Application of Nuclear Energy (INEP), University of Belgrade, Belgrade, 381, Serbia
[b] Institute of Chemistry, Slovak Academy of Sciences, Bratislava, 421, Slovakia

ARTICLE INFO

Keywords:
N-glycans
Placental glycoproteins
Placental glycans
Lectin microarray
MALDI-TOF MS

ABSTRACT

Structural changes of glycans are observed in different (patho)physiological conditions. Human placental membrane (glyco)proteins were isolated from the first and third trimester placentas of mothers at different ages. By using lectin microarray, we demonstrated that the placental membrane N-glycome contains several N-glycan groups: high mannose, asialylated and sialylated biantennary moieties, bisected, core fucosylated, fucosylated at other positions (bearing terminal and/or antennary Fuc), α2-6 and α2-3 sialylated structures. Employing MALDI-TOF MS enabled identification of over sixty different N-glycan structures in all samples, with 17 moieties exceeding the relative abundance of 2%. The major MS peaks originated from: 1) biantennary complex type N-glycan with a bisecting GlcNAc residue and 2) a core Fuc paucimannosidic and high mannose type structures M3-M9. Age of mothers and the stage of placental development affected N-glycome. The work presented in this article is the first comprehensive mass spectrometric study of the N-glycome of human placental membrane proteins. Our results may be seen as the baseline which can serve for future MALDI MS profiling of the placental membrane N-glycome in different pathophysiological conditions.

1. Introduction

Glycosylation is one of the most important co/post-translational modifications with more than 50% of proteins being glycosylated (Apweiler et al., 1999), influencing cell adhesion, receptor activation, signalling, folding, stability and protein solubility (Bieberich, 2014). Glycan-complexes termed glycoconjugates (e.g. glycoproteins, glycolipids) can be either secreted, associated with the cell membrane or located intracellularly (Laughlin and Bertozzi, 2009). Many known disease markers are membrane-bound glycoproteins (Chandler and Goldman, 2013). Although glycans modify structures of other biomolecules, the information on them is still scarce. The main reason for that is that glycan structures are not genetically coded, while the nature of glycoproteins and the complexity of glycans represent additional difficulty when it comes to the isolation of glycoproteins (i.e. membrane-integrated) and glycan deciphering (Varki, 2017).

The significance of glycomic profiling has been highlighted by recent findings that structural changes of glycans are observed in many diseases, including cancer. Therefore, glycomic profiling of the whole body (glycome mapping) in different pathophysiological states may contribute to the discovery of reliable biomarkers with disease-specific alterations. There are only a few reports on the N-glycome of membrane proteins, and all of them are dealing with cancer tissue or cancer cell lines (Wang et al., 2012; Hua et al., 2014; Sethi et al., 2014; Cheng et al., 2016; Xiang et al., 2017; Xiao et al., 2018).

The placenta is an organ positioned between mother and foetus enabling the exchange of important molecules, proteins and nutrients leading to growth and development of the healthy foetus (Brett et al., 2014). Most of the placental functions are related to its membrane (glyco)proteins (Sandovici et al., 2012). The importance of glycan composition and its effect on the proper function of proteins have been well documented, and it has been recently reported that the total plasma N-glycome changes during pregnancy (Ruhaak et al., 2014), with the changes being dependent on the stage of pregnancy (Jansen et al., 2016). Exploring glycosylation of placental proteins is important, not only for scientific reasons, but the knowledge on them can help in discovering etiology of some developmental anomalies such as pre-eclampsia, intrauterine growth retardation, ectopic pregnancies or placental cancers including choriocarcinoma (Flood-Nichols et al., 2014; Kobayashi et al., 2014; Rasanen et al., 2015; Robajac et al.,

* Corresponding author.
E-mail address: draganar@inep.co.rs (D. Robajac).
[1] Present address: Department of Physical Chemistry, Vinča Institute of Nuclear Sciences, University of Belgrade, Belgrade, 381, Serbia.

https://doi.org/10.1016/j.mad.2019.111151
Received 12 June 2019; Received in revised form 20 August 2019; Accepted 2 October 2019
Available online 04 October 2019
0047-6374/

2016). By knowing the mechanisms which underlie these processes, we can understand them better and, possibly, act to minimize their appearance or alter their outcomes. What is more, many similarities can be found between the placental growth, which follows an embryo implantation, and the spread of tumour, the most important being the establishment of an invasive phenotype (Soundararajan and Rao, 2004). In this light, change in glycosylation of placental membrane proteins that accompanies developmental (gestational) changes of placental cells (trophoblasts), could be relevant to studies of glycosylation changes during an oncogenic transformation. We were the first to report N-glycosylation profile of placental membrane proteins in healthy women, and we described how it altered in ageing and, also, during gestation. In our study, we employed DNA-sequencer assisted fluorophore-assisted carbohydrate electrophoresis (DSA-FACE) and lectin blotting (Robajac et al., 2014). To upgrade this study and to be able to identify a greater number of specific N-glycans that are commonly present on membrane proteins of human placenta, we employed mass spectrometry (MS), a major tool of the structural glycomics (Wuhrer, 2013). In parallel to the MS study of the placental membrane N-glycome and its age- and gestation-related changes, we evaluated the versatility of lectin microarray for the N-glycan profiling of the same samples.

2. Materials and methods

2.1. Human placentas

Human placentas (n = 27) were obtained from the Clinic of Gynaecology and Obstetrics "Narodni Front", Belgrade, Serbia, with the approval of both the hospital's and the INEP's ethical committees (the informed consent was obtained from each woman). The first trimester placentas (FTP) were collected after the elective termination of healthy pregnancies between 7^{th} and 12^{th} week of gestation (n = 12, the mean age of women was 32.0) and two pools were made according to the age, with the cut-off set at 35 years: younger (n = 9, the mean age 30.0) and older (n = 3, the mean age 41.0). The third trimester placentas (TTP) were taken following the full-term deliveries (n = 15, the mean age 30.0) and two groups were made with the cut-off set at 35 years: younger (n = 7, the mean age 24.0) and older (n = 8, the mean age 39.5). FTP samples were analysed as two pools, whereas TTP samples were analysed individually. Samples were labelled as follows: FTP pool from the younger age group (vp01) and FTP pool from the older age group (vp02), seven TTP samples from the younger age group (v8, v9, v12, v13, v14, v15, v16) and eight TTP samples from the older age group (v1, v2, v3, v5, v6, v7, v10, v11). Both FTP and TTP samples were obtained from healthy mothers, while the new-borns from the term deliveries were healthy and of the normal size.

2.2. Isolation of the placental cell membrane proteins

Placental cell membrane proteins were isolated as previously described (Robajac et al., 2014), after the homogenisation, differential ultracentrifugation and solubilisation using Triton X-100. Solubilised membrane proteins were further subjected to the size exclusion chromatography on Sephadex G100 and eluted with 50 mM PBS pH 7.4 (150 mM NaCl, 0.05% Triton X-100) in order to remove smaller proteins. Protein concentration in samples was determined using Bradford assay; the samples were lyophilised and kept at 4 °C until used.

2.3. Lectin microarray

The lyophilised samples were dissolved in 1 ml of distilled water, diluted in 50 mM PBS pH 7.4 to the protein concentration of 50 μg/ml, and applied to microarray slides coated with epoxysilane (NEXTERION Slide E, Schott, Germany). The samples were printed using a non-contact piezoelectric printer, sciFLEXARRAYER S1 and piezo dispense capillary PDC 90 (Scienion AG, Berlin, Germany), at a temperature of 14 °C and humidity of 60%. They were printed into 16 identical subarrays and held at 4 °C for 2 h, while unoccupied epoxy groups were blocked with 3% BSA in PBS, at 4 °C for 1 h. After the washing, the printed proteins were allowed to interact with 16 biotinylated lectins (all purchased from Vector, Burlingame, USA, except PhoSL, which was a kind gift from Dr Yuka Kobayashi), at room temperature for 1 h. Lectins, at the concentration of 25 μg/ml in PBS with 0.05% Tween 20 (PBST), were loaded into subarrays using a 16-well mask. After a thorough washing, the slides were allowed to interact with CF647-streptavidin conjugate (Biotium, Hayward, USA, 0.5 μg/ml in PBST) at room temperature for 15 min. Slides were again thoroughly washed with PBST and distilled water, and the residual water was removed by centrifugation. Dried slides were scanned using an InnoScan® 710 fluorescent scanner (Innopsys, Carbonne, France). Fluorescent signals were analysed using Mapix® 5.5.0 software (Innopsys), and only lectins with a signal-to-noise ratio (S/N) above 3 were subjected to the statistical analysis. Specific fluorescent signals were expressed in arbitrary units (A.U.). The statistical analysis was conducted only with the results obtained for TTP samples, since FTP samples were measured as two pools.

2.4. Matrix-assisted laser desorption/ionisation time-of-flight mass spectrometry (MALDI-TOF MS)

Hundred microliters of the samples (containing between 130–660 μg depending on the sample) and 1 μl of each: 1 M Tris pH 7.5, 10% SDS and 1 M dithiothreitol (DTT), were mixed and then incubated at 60 °C for 30 min. Each sample (both FTP and TTP) was prepared in duplicate and analysed separately. Further alkylation with 25 mM iodoacetamide (4.5 μl of 0.55 M IAA) in a dark, at room temperature, was performed for 30 min, and the process quenched with 10 mM DTT (1 μl of 1 M DTT). When the protein part of glycoprotein is not planned for further analysis, the samples don't have to be treated with DTT/IAA, and these steps can be omitted. N-glycans were released from the proteins using peptide: N-glycanase (PNGase) F at 37 °C overnight. For the glycan purification, porous graphitic carbon (PGC) columns were equilibrated first in 85% and then in 5% acetonitrile (ACN). Samples containing glycans were diluted in 5% ACN and loaded onto the PGC column. After washing away the unbound fraction with 5% ACN, the glycans (both neutral and those containing sialic acid, Sia-containing) were eluted with the mixture of 40% ACN and 0.1% trifluoroacetic acid, frozen and lyophilised overnight. In order to stabilise sialic acids (Sia), the glycan samples were further subjected to permethylation with iodomethane (in a ratio 1:1) in the presence of saturated NaOH in dimethyl sulfoxide, at room temperature for 30 min, with constant shaking, until a white precipitate was obtained. The reaction was terminated by neutralisation with an ice-cold 1% HCl. The permethylated glycans were further purified using C18 column, which was equilibrated with 85% ACN. The unbound molecules were washed off using water, while the permethylated glycans were eluted with 80% ACN and dried in a vacuum centrifuge. Finally, dried permethylated glycans were dissolved in 50% MeOH and 1 μl of this solution was mixed with 1μ of 2,5-dihydroxybenzoic acid matrix (in the presence of 1 mM NaOH) and analysed on MALDI-TOF mass spectrometer. MALDI-TOF MS workflow scheme is presented in Fig. 1.

The samples were analyzed in a reflection positive-ion mode on an UltrafleXtreme MALDI-TOF-MS mass spectrometer equipped with the 1000 Hz Smartbeam™-II laser and Flexcontrol software 3.4. (Bruker Daltonics, MA, USA). The instrument was calibrated using a polyethylene glycol (PEG 1500 and 8000, Sigma Aldrich), with an *m/z* range $[M + Na]^+$ from 800 to 6000. A 25 kV acceleration voltage was applied after a 110 ns extraction delay. A mass window of *m/z* 800 to 6000 was used with the suppression up to *m/z* 700. Each sample was applied onto four separate spots on the MALDI target plate, i.e. 4 times 2 000 laser shots were accumulated for each sample. MALDI MS spectra

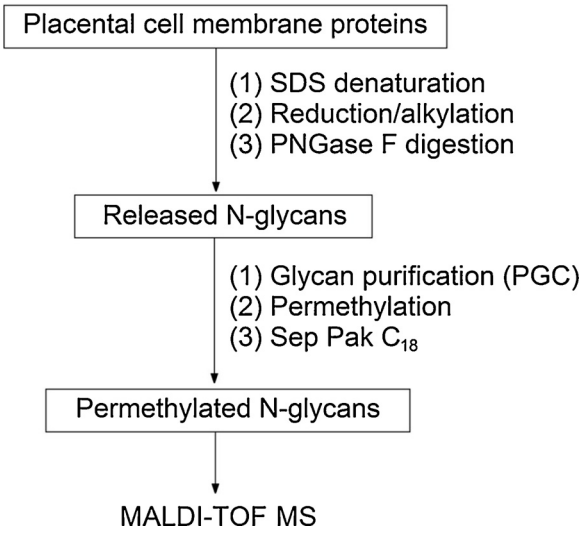

Fig. 1. Workflow scheme of the MALDI-TOF MS employed for the analysis of placental membrane N-glycome.

were acquired in a fully automated mode, using a partial sample random walk with 200 shots per raster spot. The complete MALDI MS analysis of all the samples was repeated twice. All spectra were processed and analysed by the FlexAnalysis and ProteinScape 3.0 software (Bruker Daltonics, MA, USA), though some of the signals were manually annotated with the assistance of GlycoWorkBench software. The signal intensity of each N-glycan was normalised by presenting as a percentage of total peak area (100%).

2.5. Data analysis

Statistical analysis was performed to determine possible differences between the investigated groups of samples. The results were presented as median values and percentile ranks, whereas non-parametric Mann-Whitney test was used to assess the statistically significant difference (at p-value < 0.05).

3. Results

3.1. Lectin microarray

We aimed to evaluate the versatility of the lectin microarray technique in profiling N-glycans that are covalently attached to the placental membrane proteins. Another goal was to test whether the lectin microarray can be applied to assess the age-related (mothers from different age groups) and gestation-related (first vs. the third trimester of pregnancy) alterations of the membrane N-glycome.

Nine out of sixteen tested lectins displayed the requested sensitivity, i.e. S/N above 3 (Table 1).

The strongest signals were observed in the case of Con A binding (signal intensity > 2500 A.U.) and PHA-E binding (signal intensity > 2000 A.U.) to FTP samples from younger women (Fig. 2A). These samples also displayed a moderately high binding to fucose-binding lectins (Fig. 2B): AAL (signal intensity ca. 1500 A.U.) and PhoSL (signal intensity ca. 1000 A.U.). In general, the results demonstrated that the placental membrane N-glycome contained several common N-glycopatterns: high mannose N-glycans and asialylated hybrid and biantennary N-glycans (Con A binding), bisecting GlcNAc (PHA-E binding), core fucosylated (PhoSL binding, AAL binding) and terminal and/or antennary fucosylated N-glycans (AAL binding), α2-6 sialylated (SNA binding) and α2-3 sialylated (MAL-I and MAL-II binding) N-glycans. As shown in Table 1, interaction with three lectins resulted in binding signals lower than the set threshold (PHA-L, LCA, GSL), whereas four tested lectins showed no binding at all (PNA, HHL, GNL, NPL). The age of placentae donors had a great impact on the N-glycan profile of membrane proteins in the FTP samples. The differential binding of all lectins, except MAL-II, was observed between the two pools (Fig. 2C). The most profound differences were found in the case of Con A and PHA-E (Fig. 2A). The signal intensities (i.e. the lectin binding) were always stronger in the FTP pool of younger women.

In the TTP group (Fig. 3), statistically significant differences between the younger and older mothers were found for lectins: Con A, RCA, AAL, PhoSL, SNA and MAL-II (the results for WGA and PHA-E were very close to the level of significance). There was no difference in the case of MAL-I (Fig. 3C). As a rule, membrane glycoproteins from older mothers interacted more strongly with all tested lectins than those from the younger group (Fig. 3A), which was opposite to the pattern observed in FTP samples.

To assess whether the lectin microarray could detect the gestation-related differences in N-glycoprofiles, we compared the values of lectin binding obtained for FTP and TTP samples (Fig. 4).

The glycoproteins from TTP samples always gave stronger signals of lectin binding than those from FTP samples (Fig. 4A). The significant differences between FTP and TTP were observed only in MAL-I binding (Fig. 4C), most probably due to great inter-individual variability in tested groups. Thus, the lectin microarray could detect some age-related differences in N-glycosylation pattern of placental membrane proteins, but it was not sensitive enough to detect the gestation-related differences.

3.2. MALDI-TOF MS

By employing MALDI-TOF MS we have identified 66 different N-glycan structures, which were covalently bound to human placental membrane proteins (see MALDI-TOF mass spectrum in Fig. S1), and their compositions are given in Table 2.

The N-glycans were identified on the basis of their *m/z* values, either by comparing them to the *m/z* values of known N-glycans in the serum from a healthy individual or by manually calculating their composition (Fig. S2).

The relative abundances of all detected N-glycans were calculated from the intensities of their *m/z* signals for each sample. The major *m/z* signals from all FTP and TTP samples, i.e. those with the relative abundance equal or higher than 2%, were summed up and depicted in Fig. 5, while their comparison with the control serum is presented in Fig. S2. We noticed that almost all major *m/z* signals from the placental membranes and from the human serum overlapped. The exceptions were: *m/z* 2431.16 (monosialylated biantennary N-glycan) and *m/z* 2792.38 (disialylated biantennary N-glycan), whose signal intensities in placental membrane samples were very low. The signal at *m/z* 2489.25 (nonsialylated biantennary N-glycan with bisecting GlcNAc and core Fuc) was low in the control serum, but high in the membrane samples (Fig. S2).

Similar N-glycan landscape was observed in all four groups of samples, with 17 signals exceeding the relative abundance of 2% (Fig. 5). However, there were few exceptions: i) certain neutral agalactosylated N-glycans were missing in the samples v7 (*m/z* 1171.58, 1375.68, 1661.83 and 1906.94) and v16 (*m/z* 1375.68 and 1661.83) (Table STI); ii) 18 sialylated N-glycans were missing in the samples v9, v10 and v16 (Table STII); iii) sample v14 contained several N-glycans (predominantly triantennary and tetraantennary) that were not detected in any other sample (Table STIII).

The major peaks originated from: biantennary complex type N-glycan with a bisecting GlcNAc residue and a core Fuc (NA2FB) with *m/z* 2489.25, and paucimannosidic and high mannose type structures (M3, M3F, M4) M5, M6, M7, M8 and M9 with *m/z* (1171.58, 1345.67, 1375.68) 1579.78, 1783.88, 1987.98, 2192.08 and 2396.18, respectively (Fig. 5). This is consistent with the data obtained by the DSA-FACE analysis, where M9 and NA2FB were identified as the major peaks

Table 1
An overview of lectins used for lectin microarray together with obtained signal-to-noise ratio (S/N).

Lectin (*source*)	Carbohydrate specificity	S/N
SNA (*Sambucus nigra*)	NeuNAcα2-6Gal/GalNAc	> 3
MAL-I (*Maackia amurensis*)	NeuNAcα2-3Galβ1-4GlcNAc	> 3
MAL-II (*Maackia amurensis*)	NeuNAcα2-3Galβ1-3(± NeuNAc2-6)GalNAc	> 3
ConA (*Canavalia ensiformis*)	Manα1-6(Manα1-3)Man	> 3
WGA (*Triticum vulgaris*)	GlcNAcβ1-4GlcNAc, chitin oligomers, NeuAc	> 3
RCA (*Ricinus communis*)	Galβ1-4GlcNAc	> 3
PHA-E (*Phaseolus vulgaris*)	Galβ1-4GlcNAcβ1-2Man with bisecting GlcNAc	> 3
AAL (*Aleuria aurantia*)	Fucα1-6GlcNAc, Fucα1-3(Galβ1-4)GlcNAc	> 3
PhoSL (*Pholiota squarrosa*)	Fucα1-6GlcNAc	> 3
PHA-L (*Phaseolus vulgaris*)	Tri/tetraantennary complex type N-glycans w/ terminal Gal	< 3
GSL (*Griffonia simplicifolia*)	agalactosylated tri/tetraantennary N-glycans terminating w/ GlcNAc	< 3
LCA (*Lens culinaris*)	αDGlc, αDMan in N-glycans with Fuca1-6GlcNAc	< 3
PNA (*Arachis hypogaea*)	Galβ1-3GalNAc	–
HHL (*Hippeastrum hybrid*)	High mannose type N-glycans, Manα1-3Man, Manα1-6Man	–
GNL (*Galanthus nivalis*)	High mannose type N-glycans, Manα1-3Man	–
NPL (*Narcissus pseudonarcissus*)	High mannose type N-glycans, Manα1-6Man	–

(Robajac et al., 2014). Significantly higher signal intensities for all N-glycans were measured in the sample v14 (TTP young), which is most likely due to an increased overall content of N-glycans (Table STIII).

To assess the differences in membrane N-glycome of FTP and TTP, we divided the detected N-glycans into six subclasses according to the presence of the following unique glycan motifs: i) oligomannose branches present in high mannose type N-glycans, ii) terminal sialic acid, iii) α1-6Fuc bound to the innermost GlcNAc residue (core Fuc), iv) bisecting GlcNAc residue, v) oligofucosylation, and vi) multiantennarity. The subclasses corresponding to these motifs were: 1) high mannose N-glycans (Fig. S3), 2) sialylated biantennary N-glycans, including mono- and disialylated structures (Fig. S4), 3) (core)fucosylated biantennary N-glycans (Fig. S5), 4) oligofucosylated N-glycans (i.e. those possessing 2, 3 or 4 Fuc residues) and more than 2 Fuc residues, including core Fuc, terminal Fuc or antennary Fuc (Fig. S6), 5) N-glycans bearing a bisecting GlcNAc residue – bisected N-glycans (Fig. S7) and 6) multiantennary complex type N-glycans – those having 3 or 4 antennae (Fig. S8). The relative abundances of individual N-glycans belonging to the same group were summed up independently for each of FTP and TTP samples. The obtained sums were then subjected to statistical analysis, with the aim to test whether the gestational age was in relation to the relative abundances of these six N-glycan subclasses (Fig. 6).

The content of the high mannose and oligofucosylated was significantly higher in TTP than in FTP (1 and 4 in Fig. 6) whereas the content of the bisected N-glycans (5 in Fig. 6) was found to be lower in TTP than in FTP group. Due to a high variance within the TTP group, we could not observe a significant difference in the content of the multiantennary N-glycans (6 in Fig. 6).

The age-related differences in the content of these six N-glycan subclasses were not found to be statistically significant, possibly due to large variability within the group.

4. Discussion

In our previous study, we assessed N-glycome profiles of membrane proteins isolated from human placenta, with the aid of lectin blotting and DSA-FACE (Robajac et al., 2014). The lectin blotting was done with detergent-solubilised placental membrane (glyco)proteins. DSA-FACE, on the other hand, employed capillary electrophoresis to resolve N-glycans, which were first enzymatically cleaved from membrane glycoproteins by the action of PNGase F and then fluorescently labelled on their reducing end (Robajac et al., 2014). Both these techniques suffer from certain drawbacks: i) lectin blotting is time-consuming and low throughput technique; ii) DSA-FACE is not capable to separate all glycans as unique maxima (two or more different N-glycan structures may be eluted under the same peak). The identification of N-glycans resolved by DSA-FACE was based on the comparison of their retention times with those in human serum and RNase B high mannose N-glycans. However, some of the high mannose and biantennary N-glycans have the same retention times, e.g. NA2F = M9, NA2FB = M8 (Robajac et al., 2014). Another limitation of DSA-FACE is the necessity to desialylate the samples prior to analysis. Consequently, the information regarding terminal Sia residues is lost, i.e. non-sialylated and desialylated N-glycans are eluted together (Vanhooren et al., 2008).

Compared to lectin blotting, lectin microarray is a more convenient technique that enables a high throughput N-glycome profiling (Katrlík et al., 2010). In the study presented herein, by using lectin microarray, we demonstrated that the placental membrane N-glycome contains several N-glycan groups: high mannose, asialylated and sialylated biantennary moieties, bisected, core fucosylated, fucosylated at other positions (bearing terminal and/or antennary Fuc), α2-6 and α2-3 sialylated structures. These N-glycans and/or their structural motifs were the same as previously identified using lectin blotting with LCA, PHA-E and SNA (Robajac et al., 2014). The lectin microarray enabled us to observe the differences in the content of unique N-glycans between older and younger women. The statistics was not performed in the FTP

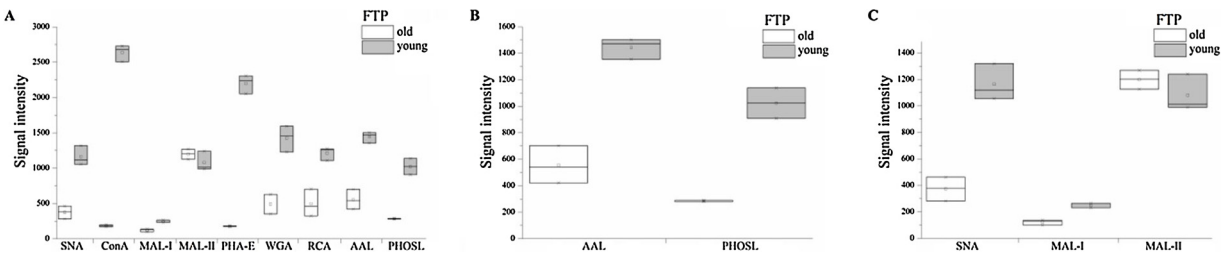

Fig. 2. Lectin microarray analysis of the membrane glycoproteins isolated from the first trimester placentas (FTP) in relation to the maternal age: A) all lectins with signal intensities above the threshold (S/N > 3), B) Fuc-specific lectins, C) Sia-specific lectins. Data are shown as the mean values of three repeated measurements.

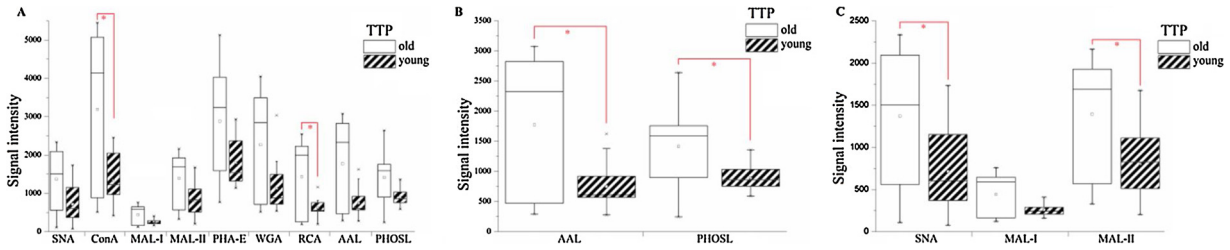

Fig. 3. Lectin microarray analysis of the membrane glycoproteins isolated from the third trimester placentas (TTP) in relation to the maternal age: A) all lectins with S/N > 3, B) Fuc-specific lectins, and C) Sia-specific lectins. *Statistically significant differences between the two groups of samples.

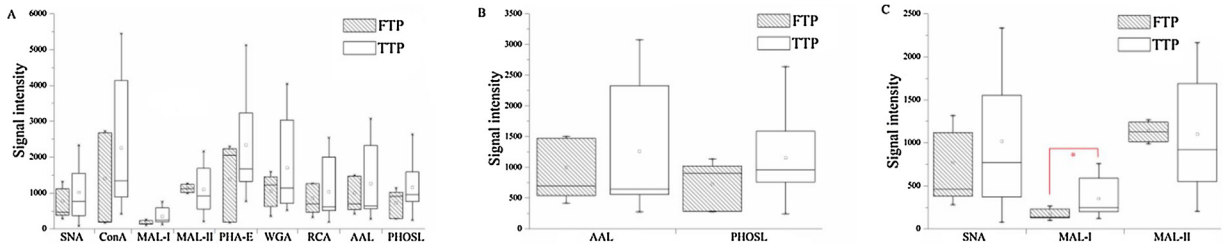

Fig. 4. Lectin microarray analysis of the membrane glycoproteins isolated from the first (FTP) and the third (TTP) trimester placentas: A) all lectins with S/N > 3, B) Fuc-specific lectins, and C) Sia-specific lectins. *Statistically significant differences between two groups of samples.

group because we made two pools of individual samples (younger and older). In spite of this, the obtained results for FTP are valuable since these pools represent average values of individual FTP samples. FTPs from the younger women consistently had a greater content of all tested N-glycan motifs, except those recognised by MAL-II lectin. The greatest difference was noticed in the content of N-glycans recognised by Con A and PHA-E. It is known that Con A has a high affinity for high mannose N-glycans (Table 1) but it also binds hybrid and biantennary N-glycans (with our without core Fuc) (Narasimhan et al., 1986). On the other side, other three lectins that were strictly specific for high mannose moieties, such as HHL, GNL and NPL, did not give any signal in the microarray, i.e. it was as if these glycans were absent from the FTP samples. Hence we suggest that the content of biantennaries is greater in the younger FTP group. The differential PHA-E binding suggested the greater content of bisected biantennaries/triantennaries in FTP from younger than in FTP from older. We have also found age-related differential content of asialylated galactosylated (RCA binding), core fucosylated and antennae/terminally fucosylated (PhoSL and AAL binding), α2,6-sialylated (SNA binding) and α2,3-sialylated (MAL-I binding) N-glycans in the two FTP groups. In our previous study we had also found the differential age-related content of core fucosylated and α2,3-sialylated N-glycans in FTPs, when we had used lectin blotting (Robajac et al., 2014). The MAL-II recognition unit, which is NeuNAcα2-3Galβ1-3(± NeuNAc2-6)GalNAc, is found exclusively on O-glycans (Geisler and Jarvi, 2011). Thus, it appears that the content of this O-glycan motif in FTPs is not age-dependent. In the third trimester placentas (TTP), we detected the greater content of six N-glycan motifs in the older group compared to the younger: biantennaries with/without core Fuc, asialylated galactosylated N-glycans, core fucosylated and antennae/terminally fucosylated, α2,6-sialylated and α2,3-sialylated N-glycans. The greatest difference was, again, noticed in the content of biantennary N-glycans. This finding is in concordance with our previous study, when we had also found the differential age-related content of core fucosylated and α2,6-sialylated N-glycans in TTPs, with the aid of lectin blotting (Robajac et al., 2014).

The gestation-related differences in N-glycan landscape of placental cell membranes almost never reached the level of statistical significance, most probably due to the great within-group variances, with an exception in α2,3-sialylated N-glycans (MAL-I binding). Thus, the lectin microarray could detect some age-related differences in N-glycosylation pattern of placental membrane proteins, but it was not sensitive enough to detect the gestation-related differences.

Although the lectin microarray is much simpler technique than lectin blotting and although it can provide a high-throughput analysis of N-glycan landscape, it suffers from a serious drawback. Namely, lectin specificities are not yet completely known and almost each lectin recognises more than one N-glycan motif. It is not impossible that lectins recognise some non-carbohydrate units on glycoproteins, as was shown for Con A, RCA, WGA and others (Komath et al., 2006). So, if we seek to find a specific biomarker, i.e. a unique N-glycan structure which is altered due to ageing or in the course of gestation, we should use an exact technique, which unequivocally identifies a glycan structure, and which does not rely on biological recognition phenomena (as these can be affected by other factors that we still do not know). In our earlier study on N-glycan landscape of human placental cell membranes, we tried to overcome the innate uncertainties coupled to identification of N-glycan motifs with lectins. We employed a technique which resolves N-glycans according to their retention time in a capillary electrophoresis system: DSA-FACE (Robajac et al., 2014). To upgrade our earlier studies (Robajac et al., 2014) and identify specific N-glycans that are commonly attached to membrane proteins of human placentae, we employed mass spectrometry, due to its indispensable role in structural glycomics (Wuhrer, 2013). Our method of choice was MALDI-TOF MS, as it is frequently used in N-glycomics (Harvey, 2011, 2012). The mass of an analysed N-glycan unambiguously provides information on its composition in terms of the content of: hexoses, N-acetylhexosamines, deoxyhexoses (Fuc), NeuNAc (Sia) etc. Hence, MS is a unique technique in the sense that it provides a direct and reliable relation between the identity of a glycan and its physical property (m/z), which is not affected by other factors. This is not true for liquid chromatography (e.g. HPLC) or capillary electrophoresis (e.g. DSA-FACE) methods, whose output depends not only on physico-chemical properties of the analyte, but also on temperature, column type, solvent systems for elution, flow-rate, efficiency of the fluorescent labelling of glycans, matrix effects, presence of detergents etc.

With the aid of MALDI-TOF MS, we identified over sixty different N-glycans in human placental membrane proteins. The mass spectra of both FTP and TTP were dominated by the bisected core-fucosylated biantennary N-glycan (NA2FB) and paucimannosidic and high mannose N-glycans: M3-M4 and M5-M9. The N-glycan repertoire consisted mostly of biantennary structures: 20 out of 66 (ca. 30%) and 6 out of 17 most abundant, i.e. those whose abundance exceeded 2% (ca. 35%)

Table 2
N-glycans analysed in placental membrane proteins by MALDI-TOF MS. Shown are obtained masses (*m/z*) together with possible composition of obtained N-glycan. In bold are given glycans whose abundance is above 2%.

m/z	N-glycan composition
1171.6	$Hex_3HexNAc_2$
1345.7	**$Hex_3HexNAc_2dHex_1$**
1375.7	$Hex_4HexNAc_2$
1416.7	$Hex_3HexNAc_3$
1579.8	**$Hex_5HexNAc_2$**
1590.8	$Hex_3HexNAc_3dHex_1$
1620.8	$Hex_4HexNAc_3$
1661.8	$Hex_5HexNAc_4$
1783.9	**$Hex_6HexNAc_2$**
1794.9	$Hex_4HexNAc_3dHex_1$
1824.9	$Hex_5HexNAc_3$
1835.9	$Hex_3HexNAc_4dHex_1$
1866.0	$Hex_4HexNAc_4$
1907.0	$Hex_3HexNAc_5$
1969.0	$Hex_4HexNAc_3dHex_2$
1982.0	$Hex_4HexNAc_3NeuNAc_1$
1988.0	**$Hex_7HexNAc_2$**
1999.0	$Hex_5HexNAc_3dHex_1$
2029.0	$Hex_6HexNAc_3$
2070.1	$Hex_5HexNAc_4$
2081.1	$Hex_3HexNAc_5dHex_1$
2111.1	$Hex_4HexNAc_5$
2156.1	$Hex_4HexNAc_3dHex_1NeuNAc_1$
2186.1	$Hex_5HexNAc_3NeuNAc_1$
2192.1	**$Hex_8HexNAc_2$**
2203.1	$Hex_6HexNAc_3dHex_1$
2244.2	**$Hex_5HexNAc_4dHex_1$**
2286.2	**$Hex_4HexNAc_5dHex_1$**
2315.2	$Hex_5HexNAc_5$
2360.2	$Hex_5HexNAc_3dHex_1NeuNAc_1$
2390.2	$Hex_6HexNAc_3NeuNAc_1$
2396.2	**$Hex_9HexNAc_2$**
2418.2	$Hex_5HexNAc_4dHex_2$
2431.2	$Hex_5HexNAc_4NeuNAc_1$
2448.3	$Hex_6HexNAc_4dHex_1$
2472.2	$Hex_4HexNAc_5NeuNAc_1$
2489.3	**$Hex_5HexNAc_5dHex_1$**
2519.3	$Hex_6HexNAc_5$
2592.3	$Hex_5HexNAc_4dHex_3$
2600.3	$Hex_{10}HexNAc_2$
2605.3	**$Hex_5HexNAc_4dHex_1NeuNAc_1$**
2663.4	**$Hex_5HexNAc_5dHex_2$**
2693.4	**$Hex_6HexNAc_5dHex_1$**
2734.4	$Hex_5HexNAc_6dHex_1$
2779.4	$Hex_5HexNAc_4dHex_2NeuNAc_1$
2792.4	$Hex_5HexNAc_4NeuNAc_2$
2837.5	$Hex_5HexNAc_5dHex_3$
2850.5	**$Hex_5HexNAc_5dHex_1NeuNAc_1$**
2867.5	$Hex_6HexNAc_5dHex_2$
2880.5	$Hex_6HexNAc_5NeuNAc_1$
2938.5	**$Hex_6HexNAc_6dHex_1$**
3041.5	$Hex_6HexNAc_5dHex_3$
3054.6	**$Hex_6HexNAc_5dHex_1NeuNAc_1$**
3142.6	**$Hex_7HexNAc_6dHex_1$**
3215.7	$Hex_6HexNAc_5dHex_4$
3228.6	$Hex_6HexNAc_5dHex_2NeuNAc_1$
3299.7	$Hex_6HexNAc_6dHex_1NeuNAc_1$
3320.7	$Hex_7HexNAc_6NeuNAc_1$
3387.7	$Hex_7HexNAc_7dHex_1$
3402.7	$Hex_6HexNAc_5dHex_3NeuNAc_1$
3503.8	**$Hex_7HexNAc_6dHex_1NeuNAc_1$**
3591.8	$Hex_8HexNAc_7dHex_1$
3664.9	$Hex_7HexNAc_6dHex_4$
3677.8	$Hex_7HexNAc_6dHex_2NeuNAc_1$
3852.0	$Hex_7HexNAc_6dHex_3NeuNAc_1$
3953.0	$Hex_8HexNAc_7dHex_1NeuNAc_1$

(Fig. 7).

The high mannose N-glycans, M5 to M9, comprised almost one-third of the most abundant N-glycans, whereas multiantennary N-glycans (tri- and tetraantennaries) comprised ca. 30% of them (Fig. 7). Though hybrid N-glycans were present in relatively great number in the total N-glycan pool (15 out of 66), none of them reached the abundance > 2%.

High mannose N-glycans are derived either from incomplete processing of N-glycans or from intracellular membrane compartments present in the membrane samples (Costa et al., 2018; Xiao et al., 2018; Xiang et al., 2017; Cheng et al., 2016; Sethi et al., 2014). Contrary to membrane proteins, high mannose glycans are not commonly attached to serum proteins (Gebrehiwot et al., 2018; Reiding et al., 2017; Clerc et al., 2016). Undifferentiated human embryonic stem cells were shown to contain large amounts of high mannose N-glycans (Montacir et al., 2017). Abundance of high mannose N-glycans is a common feature of both cancer cell lines and cancer tissues (de Leoz et al., 2011; Sethi et al., 2016; Cheng et al., 2016). MALDI TOF MS analysis of liver tissues shown that their N-glycomes were dominated by high-mannose type glycans (Cheng et al., 2016). A dominance of high mannose type structures in membrane-bound glyco(proteome) was observed in tumour cells in culture such as: HeLa (Horvat et al., 2012, 2013), CRC (Sethi et al., 2014; Holst et al., 2016), Caco 2 (Park et al., 2015) melanoma (Link-Lenczowski et al., 2018). Link-Lenczowski reported that high mannose N-glycans comprised 58% of all membrane N-glycome of melanoma cells. It was recently reported that the N-glycans on the surface of placental cytotrophoblast and syncityotrophoblast cells were mostly those of the high mannose type, whereas these glycans were much less abundant in extravillous (invasive) trophoblast cells (Chen et al., 2016).

Jansen and his co-workers performed a detailed MALDI TOF MS N-glycome analysis of sera from 29 healthy pregnant women throughout the gestation (Jansen et al., 2016). When we compared their data with data on placental membrane N-glycome, there was a high degree of similarity, i.e. the same N-glycans were present both in human plasma and in placental cell membranes, but their level of expression (relative abundance) was different. N-glycome of human plasma and few tissues/cell lines examined so far were found to be different, and there is even evidence for a differential N-glycosylation of the secreted and membrane proteins that originate from the same cells (Link-Lenczowski, 2018) or from the same tissue (Chandler and Costello, 2016). The former found that high mannose N-glycans dominated the N-glycome of melanoma cells, whereas their glycoproteins made for export bore mostly disialo and monosialo core-fucosylated diantennaries (Link-Lenczowski et al., 2018).

When comparing the gestation-related (first vs third trimester) results for the N-glycome we obtained through lectin blotting and DSA-FACE (Robajac et al., 2014) with those we obtained in the study presented herein, through the lectin microarray and MALDI-TOF MS, we found that: i) the amount of core-fucosylated (with or without bisection) and multiantennary N-glycans increased during gestation (DSA-FACE); ii) FTP had a higher content of α2,3-sialylated N-glycans (lectin blot); iii) the amount of oligofucosylated N-glycans increased during gestation (DSA-FACE and MALDI-TOF); iv) the content of high mannose N-glycans was higher in the TTPs than in the FTPs (MALDI-TOF); v) the content of bisected N-glycans was higher in FTPs than in TTPs (DSA-FACE and MALDI-TOF); vi) the content of α2,3-sialylated N-glycans is higher in TTP than in FTP (lectin microarray); vii) the content of α2,3-sialylated N-glycans is lower in TTP than in FTP (lectin blot). Based on the obtained results, we can conclude that techniques based on lectin specificities were not sensitive enough to detect all changes in the N-glycan landscape, unlike more sophisticated ones (such as MS-based).

To sum up, the gestational changes in N-glycoprofiles assessed by the lectin microarray were mainly in the content of bisected bi- and triantennaries (PHA-E binding), as well as in the content of α2,3-sialylated N-glycans (MAL-I specificity). The gestational changes in the placental N-glycome assessed by the MALDI-TOF MS were mainly in the content of high mannose, oligofucosylated and bisected N-glycans. According to the numerous studies on cancer glycomics, cancer-specific N-glycome changes in tissues and cells are the following: premature

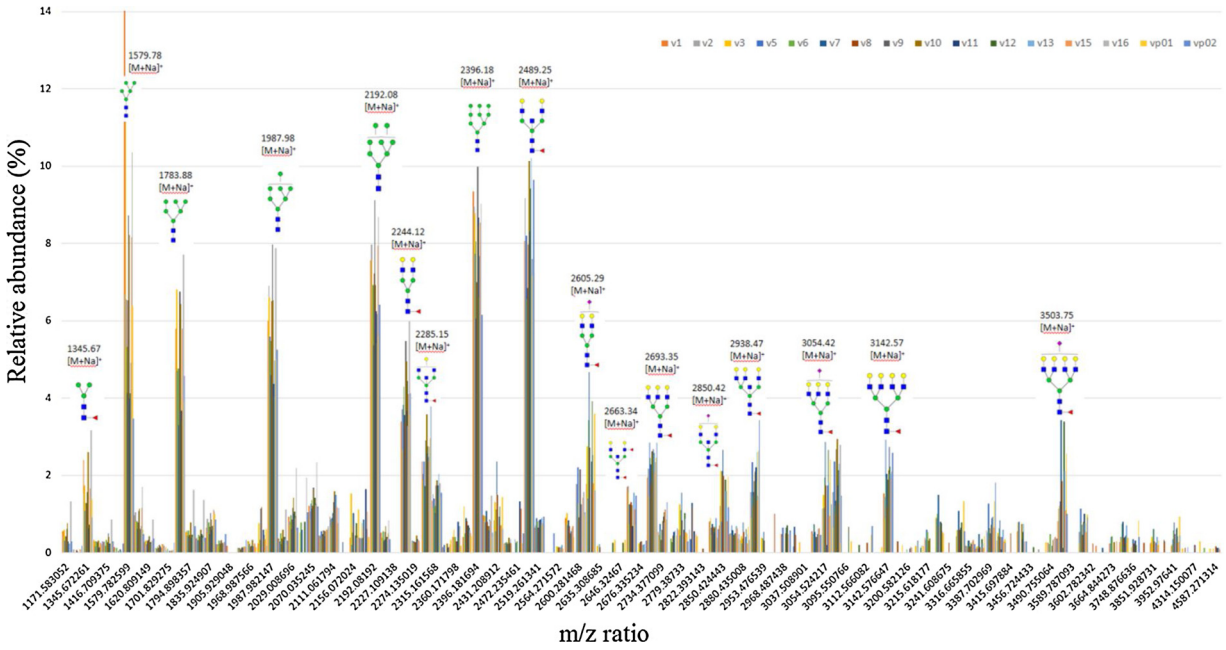

Fig. 5. The most abundant N-glycans from the placental membrane proteins. Displayed are those with the relative abundance ≥ 2% of the total N-glycans. N-glycans are presented according to the Consortium for Functional Glycomics (CFG). Different samples are shown using different colours, whereas identities of samples are shown in the upper right corner.

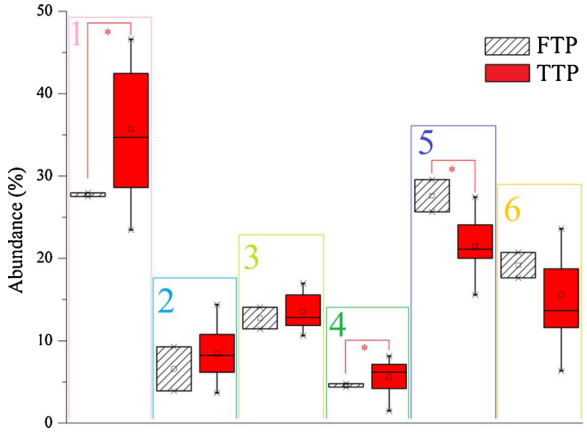

Fig. 6. The effect of the gestational age on the relative abundances of six groups of N-glycans cleaved from the human placental membrane proteins: 1- high mannose N-glycans, 2- sialylated biantennary N-glycans, 3- (core)fucosylated biantennary N-glycans, 4- highly fucosylated N-glycans, 5- bisected N-glycans, 6- multiantennary N-glycans. *Statistically significant differences between the two groups of samples.

termination of N-glycan processing (accumulation of high mannose N-glycans, altered content of bisected structures, increased branching, increased core-fucosylation and altered terminal modifications, i.e. sialylation (especially α2,3-Sia), fucosylation or the addition of LacNAc repeats (Josić et al., 2019; Wang et al., 2019; Oliveira-Ferrer et al., 2017). In other words, there is a high degree of overlapping between the published cancer-related changes and gestation-related changes in cell surface N-glycome. Trophoblast mimics malignant cell features: it has ability to invade tissues and evade host immune surveillance. Many cancers operate through reactivation of cell programmes that occurred during early stages of placentation (Costanzo et al., 2018). Signalling and metabolic pathways seen in tumours share a great degree of similarity with the pathways employed during placental development (Enninga et al., 2015). Hence, studies of placental cell glycosylation might bring out more similarities between cancer cells and (invasive) trophoblast cells, which, in turn, would result in deeper understanding of tumorigenesis.

5. Conclusion

The work presented herein, thus, confirms our previous results that N-glycome of placental membrane proteins changes during gestation (Robajac et al., 2014). The differential N-glycosylation of the placental membrane proteins in the first and third trimester of pregnancy is not serendipitous, as each alteration in glycosylation is believed to have a functional significance (Lauc et al., 2016). In the light of the fact that multiple physiological changes occur in placenta from the first to third trimester of pregnancy (Gude et al., 2004) the changes in the N-glycan composition were expected. The alterations in N-glycan repertoire expressed by a cell on its membrane proteins should be expected whenever the cell changes its degree of differentiation (Chandler and Costello, 2016).

Changes in the N-glycome of human proteins appear to be involved in almost every disease studied so far and the majority of data was derived from investigations on secretome (predominantly human plasma), leaving the N-glycome of membrane proteins largely unexplored. The work presented in this article is the first comprehensive mass spectrometric study of the N-glycome of human placental membrane proteins. Our results may be seen as the baseline which can serve for future MALDI MS profiling of the placental membrane N-glycome in different pathophysiological conditions, enabling detection of possible alteration(s) in the expression/activity of particular glycotransferase(s), caused by the epigenetic factors.

Funding

This work was supported by the bilateral cooperation grants 337-00-107/2019-09/12 and SK-SRB-18-0028 and by national grants 173042 (Ministry of Education, Science and Technological Development of the Republic of Serbia), VEGA 2/0137/18 and 2/0130/18 (Slovak Grant Agency for Science VEGA) and APVV-14-0753 (Slovak Research and Development Agency).

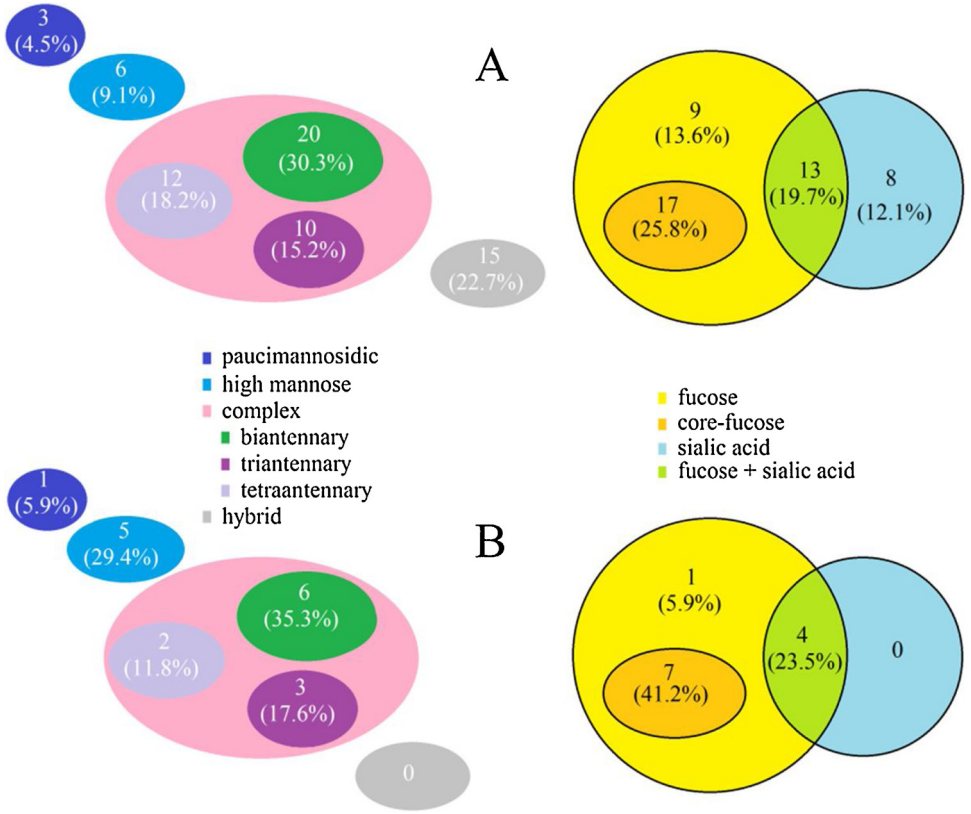

Fig. 7. Different types of N-glycans in placental membrane proteins. A) All glycan structures (as shown in the representative Fig. S1), B) glycan structures with the abundance ≥ 2%.

Acknowledgements

We are thankful to Dr Željko Miković, Dr Vesna Mandić and their technical team at the Clinic of Gynaecology and Obstetrics "Narodni Front", Belgrade, Serbia for collecting the placentas. We are very grateful to Dr Yuka Kobayashi from *J*-Oil mills, INC, for his kind gift of lectin PhoSL.

Appendix A. Supplementary data

Supplementary material related to this article can be found, in the online version, at doi:https://doi.org/10.1016/j.mad.2019.111151.

References

Apweiler, R., Hermjakob, H., Sharon, N., 1999. On the frequency of protein glycosylation, as deduced from analysis of the SWISS-PROT database. Biochim. Biophys. Acta 1473, 4–8.
Bieberich, E., 2014. Synthesis, processing, and function of N-glycans in N-glycoproteins. Adv. Neurobiol. 9, 47–70.
Brett, K.E., Ferraro, Z.M., Yockell-Lelievre, J., et al., 2014. Maternal–fetal nutrient transport in pregnancy pathologies: the role of the placenta. Int. J. Mol. Sci. 15, 16153–16185.
Chandler, K., Goldman, R., 2013. Glycoprotein disease markers and single protein-omics. Mol. Cell Proteomics 12, 836–845.
Chandler, K.B., Costello, C.E., 2016. Glycomics and glycoproteomics of membrane proteins and cell-surface receptors: present trends and future opportunities. Electrophoresis 37, 1407–1419.
Chen, Q., Pang, P.C., Cohen, M.E., et al., 2016. Evidence for differential glycosylation of trophoblast cell types. Mol. Cell Proteomics 6, 1857–1866.
Cheng, L., Gao, S., Song, X., et al., 2016. Comprehensive N-glycan profiles of hepatocellular carcinoma reveal association of fucosylation with tumor progression and regulation of FUT8 by microRNAs. Oncotarget 7, 61199–61214.
Clerc, F., Reiding, K.R., Jansen, B.C., et al., 2016. Human plasma protein N-glycosylation. Glycoconj. J. 33, 309–343.
Costa, J., Gatermann, M., Nimtz, M., et al., 2018. N-glycosylation of extracellular vesicles from HEK-293 and glioma cell lines. Anal. Chem. 90, 7871–7879.
Costanzo, V., Bardelli, A., Siena, S., et al., 2018. Exploring the links between cancer and placenta development. Open Biol. 8, 180081–180091.
de Leoz, M.L., Young, L.J., An, H.J., et al., 2011. High-mannose glycans are elevated during breast cancer progression. Mol. Cell Proteomics 10 M110.002717.
Enninga, E.A., Nevala, W.K., Holtan, S.G., et al., 2015. Immune reactivation by cell-free fetal DNA in healthy pregnancies repurposed to target tumors: novel checkpoint inhibition in cancer therapeutics. Front. Immunol. 6, 424.
Flood-Nichols, S.K., Kazanjian, A.A., Tinnemore, D., et al., 2014. Aberrant glycosylation of plasma proteins in severe preeclampsia promotes monocyte adhesion. Reprod. Sci. 21, 204–214.
Gebrehiwot, A.G., Melka, D.S., Kassaye, Y.M., et al., 2018. Healthy human serum N-glycan profiling reveals the influence of ethnic variation on the identified cancer-relevant glycan biomarkers. PLoS One 13, e0209515.
Geisler, C., Jarvis, D.L., 2011. Letter to the glyco-forum: effective glycoanalysis with Maackia amurensis lectins requires a clear understanding of their binding specificities. Glycobiology 21, 988–993.
Gude, N.M., Roberts, C.T., Kalionis, B., et al., 2004. Growth and function of the normal human placenta. Thromb. Res. 114, 397–407.
Harvey, D.J., 2012. Analysis of carbohydrates and glycoconjugates by matrix-assisted laser desorption/ionization mass spectrometry: an update for 2007–2008. Mass Spectrom. Rev. 31, 183–311.
Harvey, D.J., 2011. Analysis of carbohydrates and glycoconjugates by matrix-assisted laser desorption/ionization mass spectrometry: an update for the period 2005–2006. Mass Spectrom. Rev. 30, 1–100.
Holst, S., Deuss, A.J., van Pelt, G.W., et al., 2016. N-glycosylation profiling of colorectal cancer cell lines reveals association of fucosylation with differentiation and caudal type homebox 1 (CDX1)/villin mRNA expression. Mol. Cell Proteomics 15, 124–140.
Horvat, T., Deželjin, M., Redžić, I., et al., 2013. Reversibility of membrane N-glycome of HeLa cells upon treatment with epigenetic inhibitors. PLoS One 8, e54672.
Horvat, T., Mužinić, A., Barišić, D., et al., 2012. Epigenetic modulation of the HeLa cell membrane N-glycome. Biochim. Biophys. Acta 1820, 1412–1419.
Hua, S., Saunders, M., Dimapasoc, L.M., et al., 2014. Differentiation of cancer cell origin and molecular subtype by plasma membrane N-glycan profiling. J. Proteome Res. 13, 961–968.
Jansen, B.C., Bondt, A., Reiding, K.R., et al., 2016. Pregnancy-associated serum N-glycome changes studied by high-throughput MALDI-TOF-MS. Sci. Rep. 6, 23296.
Josić, D., Martinović, T., Pavelić, K., 2019. Glycosylation and metastases. Electrophoresis 40, 140–150.
Katrlík, J., Svitel, J., Gemeiner, P., et al., 2010. Glycan and lectin microarrays for glycomics and medicinal applications. Med. Res. Rev. 2, 394–418.
Kobayashi, Y., Masuda, K., Banno, K., et al., 2014. Glycan profiling of gestational choriocarcinoma using a lectin microarray. Oncol. Rep. 31, 1121–1126.
Komath, S.S., Kavitha, M., Swamy, M.J., 2006. Beyond carbohydrate binding: new directions in plant lectin research. Org. Biomol. Chem. 4, 973–988.

Lauc, G., Pezer, M., Rudan, I., et al., 2016. Mechanisms of disease: the human N-glycome. Biochim. Biophys. Acta 1860, 1574–1582.
Laughlin, S.T., Bertozzi, C.R., 2009. Imaging the glycome. Proc. Natl. Acad. Sci. U. S. A. 106, 12–17.
Link-Lenczowski, P., Bubka, M., Balog, C.I.A., et al., 2018. The glycomic effect of N-acetyl-glucosaminyl-transferase III overexpression in metastatic melanoma cells. GnT-III modifies highly branched N-glycans. Glycoconj. J. 35, 217–231.
Montacir, H., Freyer, N., Knöspel, F., et al., 2017. The cell-surface N-glycome of human embryonic stem cells and differentiated hepatic cells thereof. Chembiochem 18, 1234–1241.
Narasimhan, S., Freed, J.C., Schachter, H., 1986. The effect of a "bisecting" N-acetylglucosaminyl group on the binding of biantennary, complex oligosaccharides to concanavalin A, Phaseolus vulgaris erythroagglutinin (E-PHA), and Ricinus communis agglutinin (RCA-120) immobilized on agarose. Carbohydr. Res. 149, 65–83.
Oliveira-Ferrer, L., Legler, K., Milde-Langosch, K., 2017. Role of protein glycosylation in cancer metastasis. Semin. Cancer Biol. 44, 141–152.
Park, D., Brune, K.A., Mitra, A., et al., 2015. Characteristic changes in cell surface glycosylation accompany intestinal epithelial cell (IEC) differentiation: high mannose structures dominate the cell surface glycome of undifferentiated enterocytes. Mol. Cell Proteomics 14, 2910–2921.
Rasanen, J., Quinn, M.J., Laurie, A., et al., 2015. Maternal serum glycosylated fibronectin as a point-of-care biomarker for assessment of preeclampsia. Am. J. Obstet. Gynecol. 212 82.e1-9.
Reiding, K.R., Ruhaak, L.R., Uh, H.W., et al., 2017. Human plasma N-glycosylation as analyzed by matrix-assisted laser desorption/ionization fourier transform ion cyclotron resonance MS associates with markers of inflammation and metabolic health. Mol. Cell Proteomics 16, 228–242.
Robajac, D., Masnikosa, R., Vanhooren, V., et al., 2014. The N-glycan profile of placental membrane glycoproteins alters during gestation and aging. Mech. Ageing Dev. 138, 1–9.
Robajac, D., Vanhooren, V., Masnikosa, R., et al., 2016. Preeclampsia transforms membrane N-glycome in human placenta. Exp. Mol. Pathol. 100, 26–30.
Ruhaak, L.R., Uh, H.W., Deelder, A.M., et al., 2014. Total plasma N-glycome changes during pregnancy. J. Proteome Res. 13, 1657–1668.
Sandovici, I., Hoelle, K., Angiolini, E., et al., 2012. Placental adaptations to the maternal–fetal environment: implications for fetal growth and developmental programming. Reprod. Biomed. Online 25, 68–89.
Sethi, M.K., Hancock, W.S., Fanayan, S., 2016. Identifying N-glycan biomarkers in colorectal cancer by mass spectrometry. Acc. Chem. Res. 49, 2099–2106.
Sethi, M.K., Thaysen-Andersen, M., Smith, J.T., et al., 2014. Comparative N-glycan profiling of colorectal cancer cell lines reveals unique bisecting GlcNAc and α-2,3-linked sialic acid determinants are associated with membrane proteins of the more metastatic/aggressive cell lines. J. Proteome Res. 13, 277–288.
Soundararajan, R., Rao, A.J., 2004. Trophoblast' pseudo-tumorigenesis': significance and contributory factors. Reprod. Biol. Endocrinol. 2, 15.
Vanhooren, V., Laroy, W., Libert, C., et al., 2008. N-Glycan profiling in the study of human aging. Biogerontology 9, 351–356.
Varki, A., 2017. Biological roles of glycans. Glycobiology 27, 3–49.
Wang, L., Vanhooren, V., Dewaele, S., et al., 2012. Alteration of liver N-glycome in patients with hepatocellular carcinoma. Open J. Gastroenterol. 2, 1–8.
Wang, M., Zhu, J., Lubman, D.M., et al., 2019. Aberrant glycosylation and cancer biomarker discovery: a promising and thorny journey. Clin. Chem. Lab. Med. 57, 407–416.
Wuhrer, M., 2013. Glycomics using mass spectrometry. Glycoconj. J. 30, 11–22.
Xiang, T., Yang, G., Liu, X., et al., 2017. Alteration of N-glycan expression profile and glycan pattern of glycoproteins in human hepatoma cells after HCV infection. Biochim. Biophys. Acta 1861 (Pt. A), 1036–1045.
Xiao, K., Han, Y., Tian, Z., 2018. Large-scale identification and visualization of human liver N-glycome enriched from LO2 cells. Anal. Bioanal. Chem. 410, 4195–4202.